Electronic Supplementary Material (ESI) for Nanoscale.
This journal is © The Royal Society of Chemistry 2019

Selectively grown GaN nanowalls and nanogrids for photocatalysis: Growth and optical properties

Julia Winnerl,* Max Kraut, Sabrina Artmeier, and Martin Stutzmann*

Walter Schottky Institut and Physics Department, Technische Universität München, 85748 Garching, Germany

E-mail: julia.winnerl@wsi.tum.de; stutz@wsi.tum.de

Supporting information

Scanning electron microscopy of GaN nanowall arrays

In Figure 1, a high resolution 45°-tilted view scanning electron microscopy (SEM) image of a selective area grown (SAG) GaN nanowall array with a period of 500 nm and a width of 153 nm is shown. The SAG GaN nanowalls are characterized by smooth sidewalls.

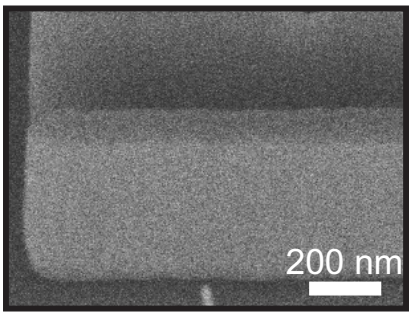

Figure 1: High resolution 45°-tilted view SEM image of a SAG GaN nanowall array with a period of 500 nm and a width of 153 nm.

In Figure 2 45°-tilted view SEM images of SAG GaN nanowall arrays with different nominal widths and a constant period of 2000 nm are illustrated. For all nominal widths, homogeneous SAG GaN nanowalls can be observed. In addition, uniform GaN nanowall SAG was achieved over a large scale (Fig. 3).

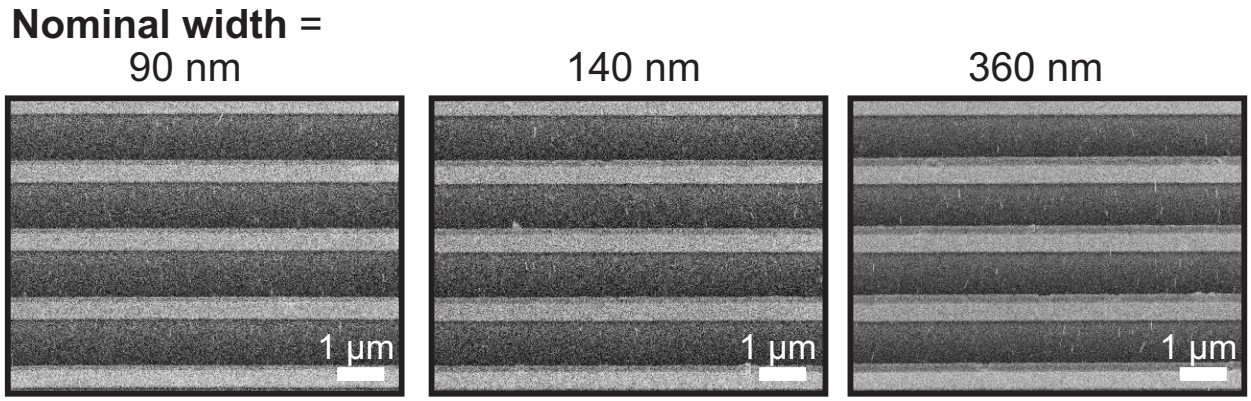

Figure 2: Tilted view (45°) SEM images of SAG GaN nanowall arrays with different nominal widths and a period of 2000 nm.

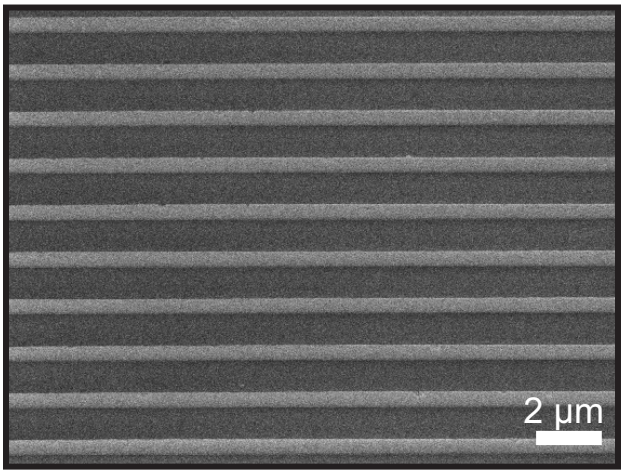

Figure 3: Tilted view (45°) SEM image of a SAG GaN nanowall array with a nominal width of 90 nm and a period of 2000 nm.

The SAG GaN nanowalls presented in the main article were grown on sapphire substrates. Besides, the successful growth of GaN nanowalls on GaN on sapphire substrates was achieved. The GaN nanowall SAG on GaN on sapphire substrates were conducted under equivalent growth conditions, i.e. a N flux of 0.363 sccm, a Ga beam-equivalent pressure of $5{\cdot}10^{-7}$ mbar

and a growth time of 90 min, with an adjusted substrate temperature of 960°. Similar results were obtained for SAG GaN nanowalls on sapphire and GaN on sapphire substrates. However, different nanowall morphologies were observed for m-plane and a-plane nanowalls. Exemplary top (left) and 45°-tilted view (right) SEM images of m-plane and a-plane SAG GaN nanowalls grown on GaN on sapphire substrates are illustrated in Figure 4(a) and (b), respectively. The m-plane nanowalls exhibit smooth side walls, whereas the side walls of the a-plane nanowalls are rough. Gačević et al. showed that, in GaN nanowire SAG, the nucleation of the GaN nanowires is driven by SAG kinetics, whereas the formation of the hexagonal nanowire shape is driven by free surface energy minimization.[1] Here, the observed differences in nanowall morphology may also be related to the minimization of the free surface energy. In the literature, a lower surface energy of m-plane than that of a-plane is predicted.[2,3] The side facets of the m-plane nanowalls are formed by the energetically favorable m-planes giving rise to smooth side walls. In contrast, the a-planes are energetically less favored than the m-planes and consequently a roughening of the side facets of the a-plane nanowalls occur to minimize the free surface energy. The observed difference in nanowall shape for a-plane nanowalls grown on sapphire and GaN substrates indicates that the GaN nanowall SAG is dominated by different processes, i.e. SAG kinetics and surface energy minimization, for the different substrates. However, further investigations are needed to properly explain these findings.

Photoluminescence spectroscopy of GaN nanowall arrays

In Figure 5(a) an exemplary photoluminescence (PL) spectrum of a SAG GaN nanowall array is plotted as a function of the energy. The spectrum can be divided in a near band edge emission of GaN (NBE), a sub band edge emission (SBE) and the yellow luminescence (YL). Note that a sharp line can be observed at 3.10 eV which is attributed to the excitation laser, i.e. $2/3 \cdot \lambda_{\text{laser}} = 399\,\text{nm}$. The YL is one order of magnitude weaker with respect to the NBE demonstrating the high crystal quality of SAG GaN nanowalls. In Figure 5(b) an exemplary

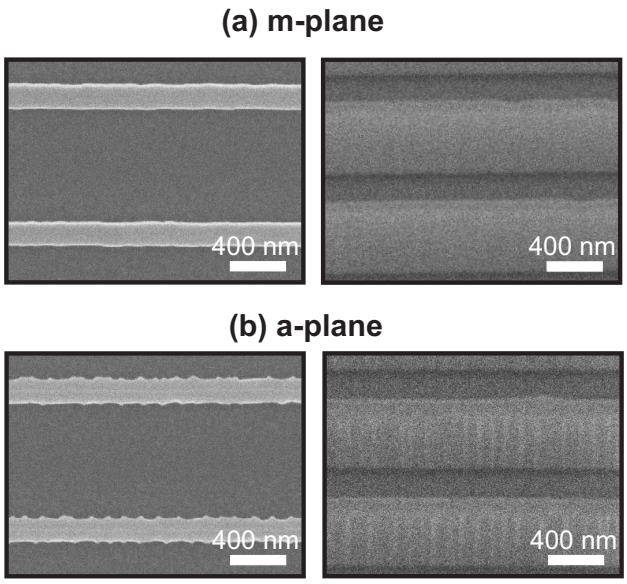

Figure 4: Top (left) and 45°-tilted view (right) SEM images of (a) m-plane GaN nanowalls and (b) a-plane GaN nanowalls grown on GaN on sapphire substrate.

PL spectrum of hollow GaN nanowalls is illustrated as a function of the energy. Similar to the GaN nanowalls (Fig. 5(a)), the SBE and YL are around one order of magnitude weaker with respect to the NBE. However, the emission peak at an energy of $\approx 3.35\,\mathrm{eV}$ is more pronounced for hollow nanowalls indicating a higher density of basal plane stacking faults. Thus, the crystal quality of GaN nanowalls is higher than that of hollow GaN nanowalls.

In Figure 6(a) low-temperature PL spectra with different widths and a constant period of 800 nm are plotted in a logarithmic scale. For all nanowall widths, the PL spectrum is characterized by a high-intensity D^0X emission and strongly suppressed defect-related emissions. Similar results were obtained for SAG GaN nanowall arrays with a period of 2000 nm (Fig. 6(b)). For increasing nanowall width an additional signal at an energy of 3.42 eV was detected for both nanowall periods and attributed to basal plane stacking faults (BSFs).[4,5] We therefore concluded that the interface quality for thin GaN nanowalls is higher than that for thick GaN nanowalls.[5]

Note that the PL intensity first decreases with increasing nanowall width and increases again for further increasing the nanowall width for both nanowall periods. This variation of the PL intensity is attributed to different incoupling efficiencies of the laser light.

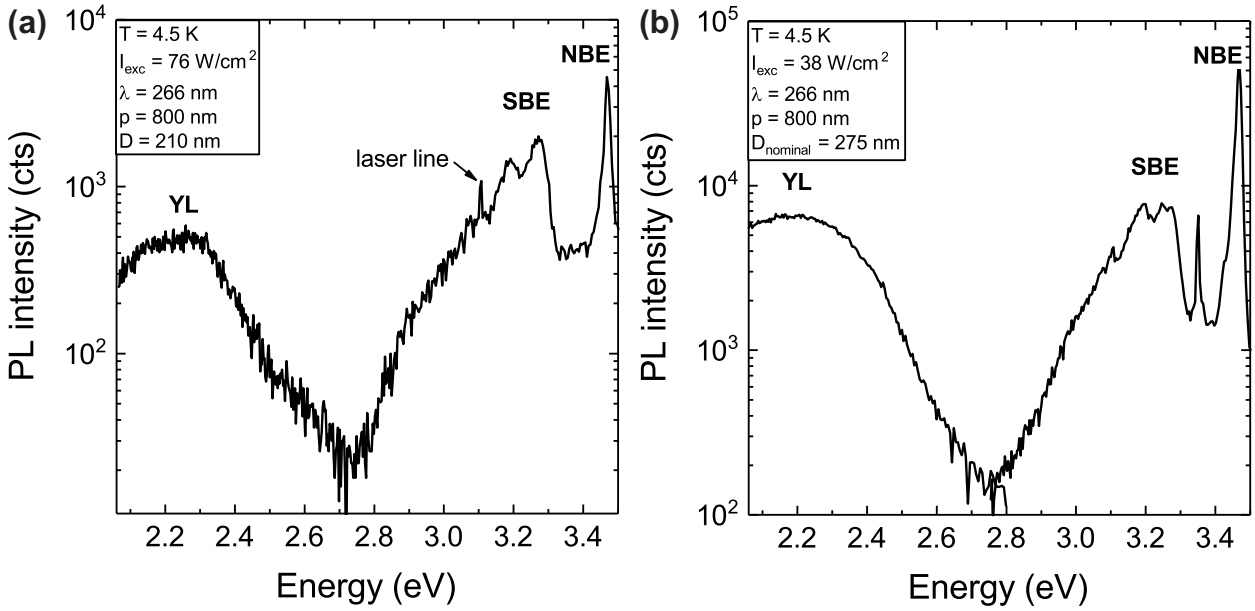

Figure 5: Low-temperature PL spectrum of SAG GaN nanowalls with (a) a width of 210 nm and (b) a nominal width of 275 nm and a constant period of 800 nm with near band edge emission (NBE), sub band egde emission (SBE) and yellow luminescence (YL).

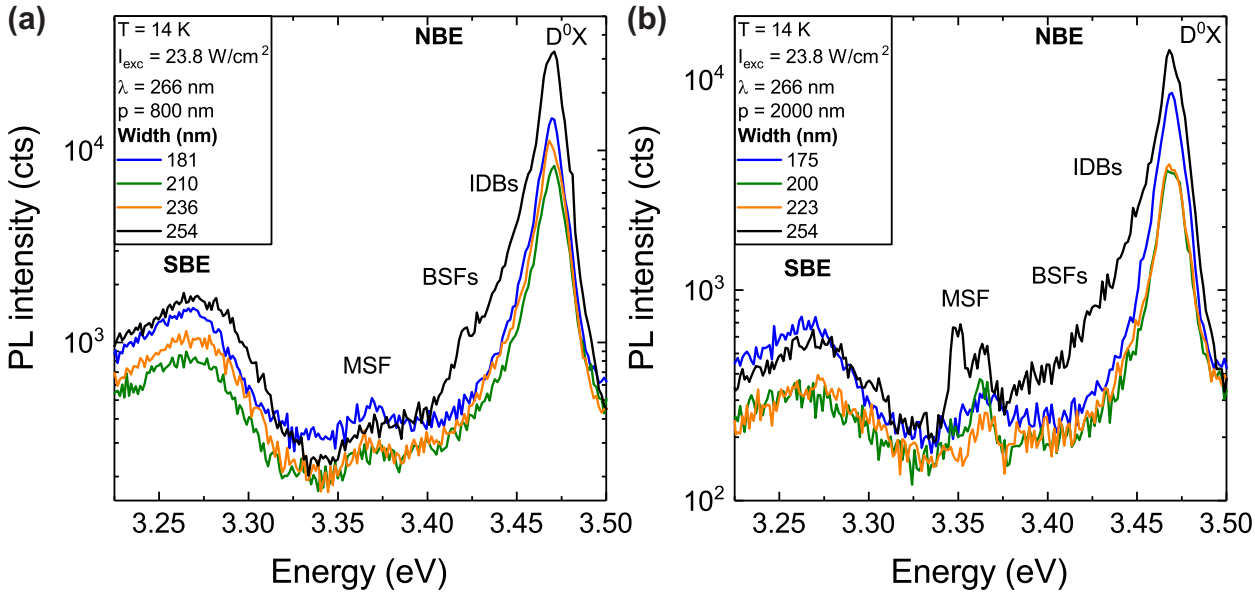

Figure 6: Low-temperature PL spectra of SAG GaN nanowalls with different widths and a constant period of (a) 800 nm and (b) 2000 nm.

Raman spectroscopy of GaN nanowalls

In Figure 7 room temperature Raman spectra of a GaN layer, SAG GaN nanowires and SAG GaN nanowalls grown on c-plane sapphire are displayed. The Raman spectra of the layer and the nanowires was vertically shifted for a better comparison. The Raman spectra show the GaN A_1(TO), E_1(TO) and E_2^{high} mode. According to M. Kuball et al., the linewidth of the E_2^{high} Raman peak is affected by the crystalline quality.[6] A full width at half maximum (FWHM) of $5.5\pm0.5\,cm^{-1}$ for the GaN layer, $3.0\pm0.5\,cm^{-1}$ for the GaN nanowires and $3.3\pm0.5\,cm^{-1}$ for the GaN nanowalls was extracted from the Raman spectra shown in Figure 7. The linewidth of the E_2^{high} peak of the GaN layer is higher than those of the GaN nanowires and nanowalls. This indicates a higher crystal quality for nanowires and nanowalls compared to layers. The similar values of the FWHM obtained for GaN nanowires and nanowalls indicate a similar crystalline quality and, thus, confirms the high quality of the GaN nanowalls.

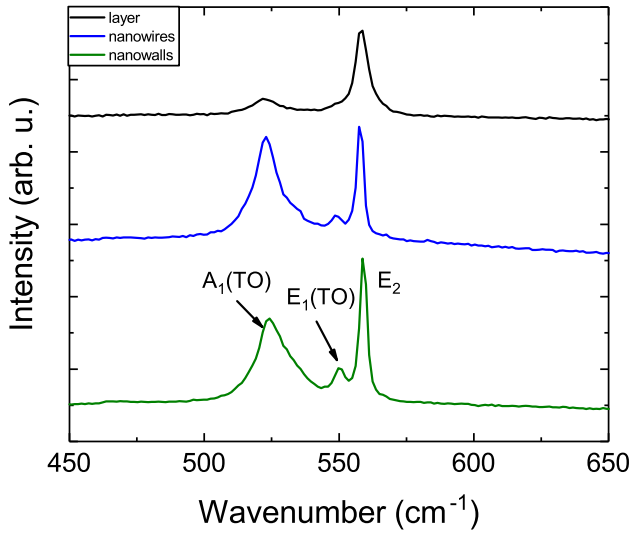

Figure 7: Room temperature Raman spectra of a GaN layer, SAG GaN nanowires and SAG GaN nanowalls.

References

(1) Gačević, Z.; Gómez Sánchez, D.; Calleja, E. Formation mechanisms of GaN nanowires grown by selective area growth homoepitaxy. *Nano Lett.* **2015**, *15*, 1117–21.

(2) Northrup, J. E.; Neugebauer, J. Theory of GaN $(10\bar{1}0)$ and $(11\bar{2}0)$ surfaces. *Phys. Rev. B* **1996**, *53*, R10477.

(3) Dreyer, C. E.; Janotti, A.; van de Walle, C. G. Absolute surface energies of polar and nonpolar planes of GaN. *Phys. Rev. B* **2014**, *89*, 081305.

(4) Corfdir, P.; Lefebvre, P.; Levrat, J.; Dussaigne, A.; Ganière, J. D.; Martin, D.; Ristić, J.; Zhu, T.; Grandjean, N.; Deveaud-Plédran, B. Exciton localization on basal stacking faults in a-plane epitaxial lateral overgrown GaN grown by hydride vapor phase epitaxy. *J. Appl. Phys.* **2009**, *105*, 043102.

(5) Hetzl, M.; Schuster, F.; Winnerl, A.; Weiszer, S.; Stutzmann, M. GaN nanowires on diamond. *Materials Science in Semiconductor Processing* **2016**, *48*, 65–78.

(6) Kuball, M. Raman spectroscopy of GaN, AlGaN and AlN for process and growth monitoring/control. *Surface and Interface Analysis* **2001**, *31*, 987–999.